Airpath Control of a SI Engine with Variable Valve Timing Actuators

Thomas Leroy, Jonathan Chauvin and Nicolas Petit

Abstract— We address the control of the airpath of a turbocharged SI engine equipped with Variable Valve Timing (VVT) actuators. VVT devices are used to produce internal exhaust gas recirculation, providing beneficial effects in terms of consumption and pollutant emissions reduction. However, VVT actuators affect the fresh air charge in the cylinders. This has an impact on the torque output (leading to driveability problems), and on the Air/Fuel Ratio (AFR) (leading to pollution peaks). To compensate these undesirable effects, a new approach is proposed. We model the intake dynamics as a first order system using a balance equation in which the VVT actuators play the role of a measured disturbance in the volumetric efficiency of the aspiration phenomenon. In view of practical implementation, two types of modeling errors are considered. We address them by an integral term and an observer. Convergence is proven. This strategy is sufficient to control the engine air mass. As a consequence, the AFR management is improved. These points are supported by experimental results.

I. INTRODUCTION AND MOTIVATIONS

Lately, Variable Valve Timing (VVT) actuators have been used in Spark Ignition (SI) engines to exploit all the possibilities of direct injection and turbocharging. This approach is of particular interest in the context of downsizing (reduction of the engine size) which has appeared as a major solution to reduce fuel consumption (see [1]).

VVT systems use electro-hydraulic mechanisms which rotate the camshaft to modify the breathing of the engine. Beneficial effects are an additional reduction of the pumping losses and an increase of the torque performance over a range wider than the one considered on conventional (fixed-valve timing) SI engine. VVT systems also allow internal exhaust gas recirculation leading to reduce Nitrogen Oxides (NO_x) and Hydrocarbons (HC) emissions [2].

One basic task in engine control consists in managing the torque output of the engine according to the driver's requests, while limiting pollutant emissions. On conventional SI engines, torque control is achieved by managing the air mass of the cylinders, while keeping the Air/Fuel Ratio (AFR) to the stoichiometric value in order to minimize exhaust emissions.

On conventional SI engines, a reference in-cylinder air mass is directly computed from the intake manifold pressure through a quasi-static relation depending on the volumetric efficiency (see [3]). Then, controlling the air mass is achieved

by controlling the intake pressure through the intake throttle. In parallel, AFR management consists of a PID controller using AFR measurement (given by an oxygen sensor situated at the engine exhaust) which is complemented by a feedforward control law to limit AFR fluctuations during torque transients [4]. The AFR controller acts upon the reference fuel mass which is sent to the injection system. The mentioned feedforward control law is designed according to a prediction of the air mass in the cylinders [5].

On SI engines equipped with VVT actuators, the in-cylinder air mass depends also on the VVT actuators positions, because these have an impact on the volumetric efficiency of the aspiration from the intake manifold into the cylinders [3], [6], [7], [8]. Their influence is modeled, but errors can not be avoided. Feedforward control law of the AFR controller is generally based, as in fixed-valve timing engine, on the air mass prediction [9]. This prediction usually has substantial errors which, unavoidably, propagate, through feedforward terms, onto the AFR management system. This issue generates pollution peaks and results in poor driveability.

We propose a simple alternative solution. Focusing on the in-cylinder air mass control problem only, we compensate two types of modeling errors with an improved control strategy. We model the intake dynamics as a first order system, using the above-mentioned volumetric efficiency related to the VVT actuators, and we consider two biases. One stands for errors in experimentally determined look-up table of the throttle actuator. The other one accounts for errors in the volumetric efficiency law. Provided that these biases are known, we obtain a one-dimensional actuated dynamics, for which the motion planning and trajectory tracking problems are already solved. From a more realistic standpoint, we propose to compensate these two biases by an integral term and an observer. Convergence is proven, using classic results from the literature on parameterized linear time-varying systems. In parallel, the AFR management system simply assumes that the reference signal for the in-cylinder air mass is tracked. Experimental results prove the relevance of this approach.

The paper is organized as follows. In Section II, we present the reference model of the intake manifold. This model consists of mass balance and aspirated flow equations. In Section III, we expose the control problem, and explain how to compute feasible trajectories to solve this motion planning problem. Section IV proposes an open-loop and a closed-loop control law for the aspirated air mass. Some preliminary assumptions (which were used for sake of simplicity in the exposition of the control design) are discussed, and the

T. Leroy (corresponding author) is a PhD Candidate in Mathematics and Control, Centre Automatique et Systèmes, École des Mines de Paris, 60, bd St Michel, 75272 Paris, France.
Email: *thomas.leroy@ensmp.fr*

J. Chauvin is with the Department of Engine Control in Institut Français du Pétrole, 1 et 4 Avenue de Bois Préau, 92852 Rueil Malmaison, France

N. Petit is with the Centre Automatique et Systèmes, École des Mines de Paris, 60, bd St Michel, 75272 Paris, France

control law is modified accordingly. An integral term and an observer are proposed. Convergence proof of the tracking error is given in Section V. In Section VI, we show experimental results obtained on a presented test bench. Finally, we conclude and give future directions in Section VII.

II. AIRPATH MODELING

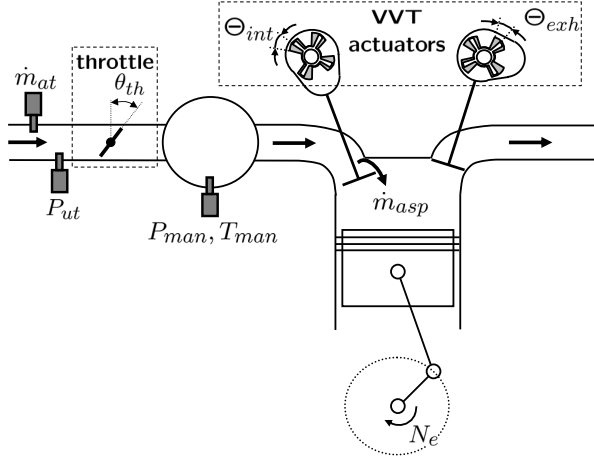### A. Balance equations for the intake manifold

Fig. 1. Airpath scheme. Intake mass air flow, $\dot{m}_{at}$, upstream throttle pressure, P_{ut}, intake manifold pressure and temperature, P_{man} and T_{man}, and engine speed, N_e, are measured by sensors. $\dot{m}_{asp}$ is the unknown aspirated mass air flow. θ_{th}, Θ_{int} and Θ_{exh} are the actuators angle positions.

Notations are given in Table I. Consider the airpath of a SI engine equipped with VVT actuators as depicted in Figure 1. In this configuration, i.e. with internal exhaust gas recirculation, the airpath has a very simple structure. It can be modeled by the intake manifold which has an inlet flow (controlled by the throttle) and an outlet flow (impacted by the VVT actuators). We consider the intake manifold as a constant volume for which the thermodynamic states (pressure, temperature, composition) are assumed spatially homogeneous. Also, we neglect time variations of temperature in this volume (following [10] and [11]), i.e. $\dot{T}_{man} = 0$. Under these assumptions, a mass balance in the intake manifold gives

$$\dot{P}_{man} = \alpha(\dot{m}_{at} - \dot{m}_{asp}) \tag{1}$$

with $\alpha \triangleq \frac{RT_{man}}{V_{man}}$. Both P_{man} and T_{man} are measured by sensors located in the intake manifold. $\dot{m}_{at}$ is the intake mass air flow. It is measured by a sensor placed upstream the throttle (see Figure 1). Respectively, $\dot{m}_{asp}$ is the mass air flow aspirated into the cylinders.

The intake mass air flow can be modeled under the form

$$\dot{m}_{at} = S_{th}f(P_{man}) - b_1 \tag{2}$$

where S_{th} is the opening throttle area. The mass flow rate $f(P_{man})$ is given in [3], under the form

$$f(P_{man}) = \kappa P_{ut} \begin{cases} P_r^{\frac{1}{\gamma}} \sqrt{\frac{2\gamma}{\gamma-1}\left(1 - P_r^{\frac{\gamma-1}{\gamma}}\right)} & \text{if } P_r > 0.528 \\ \sqrt{\gamma\left(\frac{2}{\gamma+1}\right)^{\frac{\gamma+1}{\gamma-1}}} & \text{otherwise} \end{cases} \tag{3}$$

where $\kappa \triangleq \frac{1}{\sqrt{RT_{man}}}$ and $P_r \triangleq \frac{P_{man}}{P_{ut}}$, P_{ut} is the upstream pressure from the throttle (considered as constant under atmospheric conditions), and γ is the specific heats ratio in the intake manifold. The constant bias b_1 is added to compensate modeling errors, e.g. in the experimentally determined look-up table used to transform the opening throttle area S_{th} into a throttle angle θ_{th}.

Following [3], the mass air flow through the inlet valves is modeled under the form

$$\dot{m}_{asp} = (\eta_\Phi(P_{man}) + b_2)\beta P_{man} \tag{4}$$

with $\beta \triangleq \frac{V_d}{RT_{man}}\frac{N_e}{2}$. In this equation, $\eta_\Phi(P_{man})$ is a volumetric efficiency. It depends on the intake pressure, P_{man}, and also on operating conditions such as the engine speed, N_e, and, most importantly, on the VVT actuators positions, i.e. $\Phi \triangleq (N_e, \Theta_{int}, \Theta_{exh}) \in \mathbb{R}^3$. The function $x \mapsto \eta_\Phi(x)$ is assumed to be known (through look-up table) for every values of Φ. The constant bias b_2 is added to compensate modeling errors (see [10], [12]).

TABLE I
NOMENCLATURE

Symbol	Description	Unit	Variable
b_1	Intake mass air flow bias	kg/s	
b_2	Volumetric efficiency bias	-	
$\dot{m}_{at}$	Throttle mass air flow	kg/s	y_2
$\dot{m}_{asp}$	Aspirated mass air flow	kg/s	
m_{asp}	In-cylinder air mass	kg	z
N_e	Number of crankshaft revolutions	s^{-1}	
n_{cyl}	Number of cylinders	-	
P_{man}	Intake manifold pressure	Pa	x, y_1
P_{ut}	Pressure upstream the throttle	Pa	
R	Ideal gas constant	$J/kg/K$	
S_{th}	Throttle opening area	m^2	u
T_{man}	Intake manifold temperature	K	
V_d	Total displaced volume of all the cylinders	m^3	
V_{man}	Intake manifold volume	m^3	
η_Φ	Volumetric efficiency	-	
θ_{th}	Opening throttle angle, θ_{th}	-	
Θ_{int}	Intake valve timing actuator position	$^\circ CA$	
Θ_{exh}	Exhaust valve timing actuator position	$^\circ CA$	

B. State space model and physical assumptions

Let us note $x \triangleq P_{man}$ and $u \triangleq S_{th}$ the state and the control variable of our system respectively. The measurements are $y_1 \triangleq x$ and $y_2 \triangleq \dot{m}_{at}$. Gathering equations (1), (4) and (2), one can write

$$\dot{x} = \alpha(uf(x) - b_1 - (\eta_\Phi(x) + b_2)\beta x) \tag{5}$$

By definition (3), $f : \mathbb{R} \to \mathbb{R}$ is a positive decreasing function. Physically, $\eta_\Phi : \mathbb{R} \to \mathbb{R}$ is a positive increasing function.

Due to physical limitations of the engine, the constants α and β are bounded. We note $\alpha \in [\underline{\alpha}, \overline{\alpha}] > 0$ and $\beta \in [\underline{\beta}, \overline{\beta}] > 0$ and consider $\dot{\alpha} = \dot{\beta} = 0$. Further, the volumetric efficiency η is also bounded, i.e. $(\eta_\Phi(x) + b_2) \in [\underline{\eta}; \overline{\eta}]$. Its derivative η'_Φ is also positive and bounded.

III. CONTROL PROBLEM

A. Air mass control

Our goal is to control the air mass aspirated into the cylinders. Three actuators have an influence on this variable: the throttle, the intake VVT and the exhaust VVT (see Figure 1). In the presented study, we control the air mass through the throttle, taking into account VVT variations which are considered as measured disturbances. VVT management is presented in [9]. Since the throttle permits to control the intake manifold pressure, we turn any air mass set point into an intake pressure set point. For that, we define a function which relates the aspirated air mass (noted z) and the intake manifold pressure, x, under the form $z \triangleq \Psi(x, b_2)$. Besides, z can also be computed by integrating the mass air flow, $\dot{m}_{asp}$, over one period $\Delta t = \frac{2}{N_e n_{cyl}}$, i.e. $z = \int_0^{\Delta t} \dot{m}_{asp} dt$. Considering (4) as a steady state relation, the Ψ function is defined by the averaging formula

$$z = \Psi(x, b_2) \triangleq (\eta_\Phi(x) + b_2)\beta x \Delta t \qquad (6)$$

B. Reference trajectories

In vehicle applications, the driver prescribes a torque set point to the control system through the acceleration pedal. This information is directly transformed into an aspirated air mass set point, z^{sp}, using a look-up table which is experimentally determined on the test bench under steady state conditions. This yields $z^{sp} \triangleq \text{map}(T_q^{sp}, N_e)$.

To reach this desired set point, we propose a motion planning based method. Airpath transients can be achieved by computing a feasible air mass trajectory. Inversion of the averaging formula (6) yields

$$x^{sp} \triangleq \Psi^{-1}(z^{sp}, b_2) = \Psi^{-1}(\text{map}(T_q^{sp}, N_e), b_2) \qquad (7)$$

The airpath has a first order dynamics (5). Therefore, this trajectory must be at least one time differentiable. In practice, this minimal smoothness requirement is guaranteed by a low-pass filtering of the torque set point, T_q^{sp}.

Since Ψ is a continuous function, x^{sp} has the same continuity and differentiability properties as z^{sp}. However, the bias b_2 is unknown, and the trajectory x^{sp} cannot be explicitly computed. To compensate this lack of information, we use an observer to reconstruct b_2. We note this estimate $\hat{b}_2$. The generated trajectory to be followed is then

$$x^r \triangleq \Psi^{-1}(\text{map}(T_q^{sp}, N_e), \hat{b}_2) \qquad (8)$$

In the following, we assume that, as a consequence of the discussed properties of the reference trajectories derivation, x^r is smooth and bounded and that $\dot{x}^r$ is bounded. The mentioned observer is presented in the next section.

IV. CONTROL SOLUTIONS

This section presents control methods guaranteeing tracking of the pressure trajectory (8).

System (5) is fully actuated and invertible. Provided that the biases b_1 and b_2 are known, for any smooth trajectory, one can easily compute an open-loop control law. As will be explained in § IV-A, this is, in theory, sufficient to guarantee tracking due to the open-loop stability of (5). When neither b_1 nor b_2 are known, a closed-loop law based on an observer can be considered. This is the topic addressed in § IV-B. Convergence can be proven, as will be shown in Section V.

A. Open-loop control when the biases are known

We consider that the biases b_1 and b_2 are known. Consider the following open-loop control law

$$u = \frac{1}{f(x)}\left(\frac{\dot{x}^r}{\alpha} + b_1 + (\eta_\Phi(x^r) + b_2)\beta x^r\right) \qquad (9)$$

After substitution in (5), we obtain

$$\dot{x} = \dot{x}^r + \alpha\beta((\eta_\Phi(x^r) + b_2)x^r - (\eta_\Phi(x) + b_2)x) \qquad (10)$$

Let $e \triangleq x - x^r$ be the error between the measurement and the reference pressure. Let $h : \mathbb{R} \rightarrow \mathbb{R}$ be the increasing continuous function on $\mathcal{I} = [x^{\min}; x^{\max}]$ defined by $h_\Phi(x) \triangleq \eta_\Phi(x)x$. From the intermediate value theorem, there exists one real c in $[\underline{x}; \overline{x}] \subset \mathcal{I}$, where $\underline{x} = \min(x, x^r)$ and $\overline{x} = \max(x, x^r)$, such that

$$h_\Phi(\underline{x}) - h_\Phi(\overline{x}) = h'_\Phi(c)(\underline{x} - \overline{x}) \qquad (11)$$

In (11), c depends on $x(t)$ and $x^r(t)$. More precisely, we can represent it as a time-varying function, depending on the initial condition of x that we shall denote λ. Using (11) in (10), we obtain

$$\dot{e} = -\alpha\beta(h'_\Phi(c(t, \lambda)) + b_2)e$$

Yet, $h'_\Phi(c(t, \lambda)) + b_2 = \eta'_\Phi(c(t, \lambda))c(t, \lambda) + \eta_\Phi(c(t, \lambda)) + b_2 \geq \underline{\eta}$ thanks to bounds given in § II-B. Then, the following proposition holds.

Proposition 1. *Consider system (5) and some smooth reference trajectory x^r. The open-loop control law (9) (which uses known values of b_1 and b_2) guarantees that the tracking error e exponentially converges towards 0 when $t \rightarrow \infty$.*

B. Closed-loop control in the case of unknown biases

In a more realistic setup, we consider that the biases b_1 and b_2 are not known. To compensate this missing information, we use an observer (defined in (13)) as an estimate of b_2. Further, to compensate b_1, we add an integral term in the feedback law aiming at tracking the reference trajectory x^r. This leads us to consider the following control law

$$\begin{aligned} u = &\; \frac{1}{f(x)}\left(\frac{1}{\alpha}(\dot{x}^r - k_p(x - x^r) - k_i \int_0^t (x - x^r)dt)\right. \\ &\left. + (\eta_\Phi(x^r) + \hat{b}_2)\beta x^r\right) \end{aligned}$$
$$\qquad (12)$$

with $k_p > 0$ and $k_i > 0$.

A nonlinear observer based on pressure measurement can be considered under the form

$$\begin{cases} \dot{\hat{x}} &= \alpha(y_2 - (\eta_\Phi(x) + \hat{b}_2)\beta\hat{x}) + \alpha\beta l_1(x - \hat{x}) \\ \dot{\hat{b}}_2 &= -\alpha\beta\hat{x}l_2(x - \hat{x}) \end{cases} \tag{13}$$

where $l_1 > 0$, $l_2 > 0$ are two tuning gains.

V. CONVERGENCE PROOF

We now prove convergence of the observer-controller presented in § IV-B. In the following, $\|\cdot\|$ is the Euclidian norm, and, for any vector valued function f, $\|f\|_\infty$ denotes $\sup_{t \geq 0} \|f(t)\|$.

A. Error dynamics

We note the observation errors $\tilde{x} \triangleq x - \hat{x}$ and $\tilde{b}_2 \triangleq b_2 - \hat{b}_2$,

$$\begin{cases} \dot{\tilde{x}} &= -\alpha\beta(\eta_\Phi(x) + b_2 + l_1)\tilde{x} - \alpha\beta\hat{x}\tilde{b}_2 \\ \dot{\tilde{b}}_2 &= \alpha\beta\hat{x}l_2\tilde{x} \end{cases} \tag{14}$$

Consider

$$V(\tilde{x}, \tilde{b}_2) \triangleq \frac{1}{2} \|\tilde{x}\|^2 + \frac{1}{2l_2} \left\|\tilde{b}_2\right\|^2 \tag{15}$$

Differentiation with respect to time leads to

$$\begin{aligned} \dot{V}(\tilde{x}, \tilde{b}_2) &= \tilde{x}\dot{\tilde{x}} + \frac{1}{l_2}\tilde{b}_2\dot{\tilde{b}}_2 \\ &= -\alpha\beta(\eta_\Phi(x) + b_2 + l_1)\tilde{x}^2 \leq 0 \end{aligned}$$

Semi-negativeness of this last expression is directly obtained from assumptions given in § II-B, together with $l_1 > 0$. Since V is decreasing, then $\tilde{x}$ and $\tilde{b}_2$ are bounded. We note

$$\|\tilde{x}\|_\infty < \infty \quad \text{and} \quad \left\|\tilde{b}_2\right\|_\infty < \infty \tag{16}$$

After substitution of (12) in (5), we obtain

$$\begin{aligned} \dot{x} &= \dot{x}^r - k_p(x - x^r) - k_i \int_0^t (x - x^r)dt - \alpha b_1 \\ &\quad + \alpha\beta((\eta_\Phi(x^r) + \hat{b}_2)x^r - (\eta_\Phi(x) + b_2)x) \end{aligned}$$

Note $e \triangleq x - x^r$ the error between the measurement and the reference pressure, and ι the integral term, i.e. $\dot{\iota} = -k_i e$. Using (11), the error dynamics can be written under the state space form

$$\begin{cases} \dot{e} = -(k_p + \alpha\beta(h'_\Phi(c(t,\lambda)) + b_2))e + \iota - \alpha(\beta x^r \tilde{b}_2 + b_1) \\ \dot{\iota} = -k_i e \end{cases} \tag{17}$$

Consider the variable (which can be interpreted as the asymptotic value of the integrator, once convergence is proven)

$$\omega = \alpha(\beta x^r \tilde{b}_2 + b_1) \tag{18}$$

and note $\tilde{\iota} = \iota - \omega$. The error dynamics (17) takes the form of a forced parameterized Linear Time-Varying (LTV) multivariable system,

$$\dot{X}_c = \mathcal{A}(t,\lambda)X_c + v(t) \tag{19}$$

with $X_c \triangleq (e \ \tilde{\iota})^T$, $v(t) \triangleq (0 \ \dot{\omega})^T$ and

$$\mathcal{A}(t,\lambda) \triangleq \begin{pmatrix} -k_p - \alpha\beta(h'_\Phi(c(t,\lambda)) + b_2) & 1 \\ -k_i & 0 \end{pmatrix}$$

In (19), the matrix $\mathcal{A}(t,\lambda)$ is impacted by the control gains k_p and k_i, while the forcing term $v(t)$ is due to observation error. To prove convergence of the pressure to the reference trajectory (which is our main objective), we show that (19) is λ-Uniformly Globally Asymptotically Stable (λ-UGAS). For that purpose, we will show that the unforced system

$$\dot{X}_c = \mathcal{A}(t,\lambda)X_c \tag{20}$$

is λ-Uniformly Globally Exponentially Stable (λ-UGES) and show some decay property of the forcing term $v(t)$.

B. Proof of exponential stability

The multivariable system (20) belongs to a class of parameterized LTV systems studied in [13]. In the following, we are going to use an important result.

Theorem 1. *(λ-UGES of parameterized LTV systems, Loría-Panteley [13]) Consider the parameterized LTV multivariable system (21) under the following form*

$$\begin{pmatrix} \dot{e} \\ \dot{\theta} \end{pmatrix} = \begin{pmatrix} A(t,\lambda) & B(t,\lambda)^T \\ -C(t,\lambda) & 0 \end{pmatrix} \begin{pmatrix} e \\ \theta \end{pmatrix} \tag{21}$$

where $e \in \mathbb{R}^n$, $\theta \in \mathbb{R}^m$, $A(t,\lambda) \in \mathbb{R}^{n \times n}$, $B(t,\lambda) \in \mathbb{R}^{m \times n}$, $C(t,\lambda) \in \mathbb{R}^{m \times n}$, $\lambda \in \mathcal{D} \subset \mathbb{R}^l$, and n, m, l are some integers. Assume that the following two properties hold.

Assumption 1. *There exists $\phi_M > 0$ such that for all $t \geq 0$ and for all $\lambda \in \mathcal{D}$, $\max\left\{\|B(t,\lambda)\|, \left\|\frac{\partial B(t,\lambda)}{\partial t}\right\|\right\} \leq \phi_M$.*

Assumption 2. *There exist symmetric matrices $P(t,\lambda)$ and $Q(t,\lambda)$ such that*

$$\begin{cases} C(t,\lambda)^T &= P(t,\lambda)B(t,\lambda)^T \\ -Q(t,\lambda) &= A(t,\lambda)^T P(t,\lambda) + P(t,\lambda)A(t,\lambda) + \dot{P}(t,\lambda) \end{cases}$$

There exist p_m, q_m, p_M and $q_M > 0$ such that, for all $(t,\lambda) \in \mathbb{R}_{\geq 0} \times \mathcal{D}$, $p_m I \leq P(t,\lambda) \leq p_M I$ and $q_m I \leq Q(t,\lambda) \leq q_M I$.

Then, the system is λ-UGES if and only if $B(t,\lambda)$ is λ-uniform persistency of excitation, i.e. there exists μ, $T > 0$ such that $\int_t^{t+T} B(\tau,\lambda)B(\tau,\lambda)^T d\tau \geq \mu I \quad \forall t$.

Consider system (20) with $\mathcal{D} = \mathbb{R}$, $n = 1$, $m = 1$. We have $A(t,\lambda) = -k_p - \alpha\beta(h'_\Phi(c(t,\lambda)) + b_2)$, $B(t,\lambda) = 1$ and $C(t,\lambda) = k_i$. Then, Assumption 1 is easily enforced with $\phi_M = 1$.

Moreover, let $P(t,\lambda) = k_i$ and $Q(t,\lambda) = 2k_i(k_p + \alpha\beta(h'_\Phi(c(t,\lambda))+b_2))$ with k_p, k_i, α, $\beta > 0$. By noticing that $h'_\Phi(c(t,\lambda)) + b_2$ is bounded, it follows that Assumption 2 is also verified. Finally, the λ-uniform persistency of excitation is readily proven with $\mu = T = 1$. We can now conclude and state the following result.

Proposition 2. *The parameterized LTV multivariable system (20) is λ-UGES.*

C. Proof of asymptotic stability

Now, consider the forced system (19). The analytic solution of the differential equation is

$$X_c(t) = \phi(t, 0, \lambda) X_c(0) + \int_0^t \phi(t, \tau, \lambda) v(\tau) d\tau$$

where ϕ is the transition matrix of the system. Since system (20) is λ-UGES, there exists $k, \gamma > 0$, independent of λ, such that $\forall t, \tau > 0$, $\|\phi(t, \tau, \lambda)\| \leq k e^{-\gamma(t-\tau)}$. Then, a bound on $X_c(t)$ can be easily obtained by

$$
\begin{aligned}
\|X_c(t)\| &\leq k e^{-\gamma t} \|X_c(0)\| + \int_0^t k e^{-\gamma(t-\tau)} \|v(\tau)\| d\tau \\
&\leq k e^{-\gamma t} \|X_c(0)\| + \mathcal{I}_1(t_1, t) + \mathcal{I}_2(t_1, t)
\end{aligned}
$$

where $\mathcal{I}_1(t_1, t) = k \int_0^{t_1} e^{-\gamma(t-\tau)} \|v(\tau)\| d\tau$ and $\mathcal{I}_2(t_1, t) = k \int_{t_1}^t e^{-\gamma(t-\tau)} \|v(\tau)\| d\tau$ and $0 \leq t_1 \leq t$. One can separately evaluate the two quantities $\mathcal{I}_1$ and $\mathcal{I}_2$.

$$
\begin{aligned}
\mathcal{I}_1(t_1, t) &= k \int_0^{t_1} e^{-\gamma(t-t_1)} e^{-\gamma(t_1-\tau)} \|v(\tau)\| d\tau \\
&\leq \frac{k}{\gamma} e^{-\gamma(t-t_1)} \|v\|_\infty (1 - e^{-\gamma t_1}) \\
\mathcal{I}_2(t_1, t) &= k \int_{t_1}^t e^{-\gamma(t-\tau)} \|v(\tau)\| d\tau \\
&\leq k \sup_{\tau \in [t_1; +\infty[} \|v(\tau)\| \int_{t_1}^t e^{-\gamma(t-\tau)} d\tau \\
&\leq \frac{k}{\gamma} \sup_{\tau \in [t_1; +\infty[} \|v(\tau)\|
\end{aligned}
$$

To obtain a bound on X_c, we use $t_1 = \frac{t}{2}$ and derive

$$
\begin{aligned}
\|X_c(t)\| &\leq k e^{-\gamma t} \|X_c(0)\| + \frac{k}{\gamma} \|v\|_\infty (e^{-\gamma \frac{t}{2}} - e^{-\gamma t}) \\
&+ \frac{k}{\gamma} \sup_{\tau \in [\frac{t}{2}; +\infty[} \|v(\tau)\|
\end{aligned}
\tag{22}
$$

Thanks to this inequality, convergence of $X_c(t)$ towards 0 can be guaranteed, provided the following two conditions hold

$$
\begin{cases}
\|v\|_\infty & < \quad \infty \quad \text{(a)} \\
\lim_{t \to \infty} \sup_{\tau \in [\frac{t}{2}; +\infty[} \|v(\tau)\| & = \quad 0 \quad \text{(b)}
\end{cases}
$$

We will now prove that this is indeed the case. The norm of the forcing term can be computed from (18),

$$\|v(t)\| = \|\dot{w}(t)\| = \alpha\beta \left\| \dot{x}^r(t) \tilde{b}_2(t) + x^r(t) \dot{\tilde{b}}_2(t) \right\| \tag{23}$$

From the observer dynamics (14), we have $\dot{\tilde{b}}_2(t) = \alpha\beta \hat{x}(t) l_2 \tilde{x}(t)$. In addition, note $\hat{x}(t) \triangleq x(t) - \tilde{x}(t)$, then

$$
\begin{aligned}
\|v(t)\| &= \alpha\beta \left\| \dot{x}^r \tilde{b}_2 + \alpha\beta l_2 x^r x \tilde{x} - \alpha\beta l_2 x^r \tilde{x}^2 \right\| \\
&\leq q(t) + l_2 r(t) + l_2 s(t) \|x\|
\end{aligned}
\tag{24}
$$

with $q(t) \triangleq \alpha\beta \|\dot{x}^r\| \|\tilde{b}_2\|$, $r(t) \triangleq \alpha^2\beta^2 \|x^r\| \|\tilde{x}\|^2$ and $s(t) \triangleq \alpha^2\beta^2 \|x^r\| \|\tilde{x}\|$. Yet, $\tilde{b}_2$ and $\tilde{x}$ are bounded, as we know from (16) and, by assumption, x^r and $\dot{x}^r$ are also bounded. We can easily deduce that $q(t)$, $r(t)$ and $s(t)$ are also bounded, $\|q\|_\infty < \infty$, $\|r\|_\infty < \infty$ and $\|s\|_\infty < \infty$. Further, to guarantee that (a) holds, we will prove that x is also bounded. Conservatively, (22) yields

$$\|X_c(t)\| \leq k e^{-\gamma t} \|X_c(0)\| + \frac{k}{\gamma}(1 + e^{-\gamma \frac{t}{2}} - e^{-\gamma t}) \|v\|_\infty$$

Using (24) we obtain

$$
\begin{aligned}
\|X_c(t)\| &\leq k e^{-\gamma t} \|X_c(0)\| + \frac{k}{\gamma}(1 + e^{-\gamma \frac{t}{2}} - e^{-\gamma t}) \\
&* (\|q\|_\infty + l_2 \|r\|_\infty + l_2 \|s\|_\infty \|x\|_\infty)
\end{aligned}
\tag{25}
$$

Yet, $\|x\| = \|x^r + e\| \leq \|x^r\| + \|e\| \leq \|x^r\| + \|X_c\|$ and then, simply,

$$\|x\|_\infty \leq \|x^r\|_\infty + \|X_c\|_\infty \tag{26}$$

From (26), inequality (25) leads to

$$
\begin{aligned}
\|X_c\|_\infty &\leq k \|X_c(0)\| + \frac{2k}{\gamma}(\|q\|_\infty + l_2 \|r\|_\infty \\
&+ l_2 \|s\|_\infty \|X_c\|_\infty + l_2 \|s\|_\infty \|x^r\|_\infty)
\end{aligned}
$$

and, finally, to

$$
\begin{aligned}
&\|X_c\|_\infty \left(1 - l_2 \frac{2k}{\gamma} \|s\|_\infty\right) \\
&\leq k \|X_c(0)\| + \frac{2k}{\gamma}(\|q\|_\infty + l_2 \|r\|_\infty + l_2 \|s\|_\infty \|x^r\|_\infty)
\end{aligned}
\tag{27}
$$

Bounds on $\|\tilde{x}\|_\infty$ and $\left\|\tilde{b}_2\right\|_\infty$ can be obtained from the definition of the candidate Lyapunov function (15) and its decreasingness. In facts, one easily derives

$$
\begin{aligned}
\|\tilde{x}\|_\infty &\leq \sqrt{\|\tilde{x}(0)\|^2 + \frac{1}{l_2} \left\|\tilde{b}_2(0)\right\|^2} \\
\text{and} \quad \left\|\tilde{b}_2\right\|_\infty &\leq \sqrt{l_2 \|\tilde{x}(0)\|^2 + \left\|\tilde{b}_2(0)\right\|^2}
\end{aligned}
\tag{28}
$$

Let us study inequality (27) when l_2 tends towards 0. On the left hand-side, we have

$$\lim_{l_2 \to 0} l_2 \frac{2k}{\gamma} \|s\|_\infty = 0$$

while, on the right hand-side,

$$
\begin{aligned}
&\lim_{l_2 \to 0}(\|q\|_\infty + l_2 \|r\|_\infty + l_2 \|s\|_\infty \|x^r\|_\infty) \\
&= \alpha\beta \|\dot{x}^r\|_\infty \left\|\tilde{b}_2\right\|_\infty + \alpha^2\beta^2 \|x^r\|_\infty \left\|\tilde{b}_2(0)\right\|_\infty^2
\end{aligned}
$$

Then, for l_2 small enough, one can derive another more conservative inequality

$$
\begin{aligned}
&\tfrac{1}{2} \|X_c\|_\infty \leq k \|X_c(0)\| \\
&+ \frac{4k}{\gamma}\left(\alpha\beta \|\dot{x}^r\|_\infty \left\|\tilde{b}_2\right\|_\infty + \alpha^2\beta^2 \|x^r\|_\infty \left\|\tilde{b}_2(0)\right\|_\infty^2\right)
\end{aligned}
$$

It follows that $\|X_c\|_\infty < \infty$, and, from (26),

$$\|x\|_\infty < \infty \tag{29}$$

The condition (a) is easily obtained from (29) and (24).

Let us now focus on the second condition (b). Inequality (28) shows that both $\tilde{x}$ and $\tilde{b}_2$ are bounded (as we already know it from the function V property). Further, we can deduce from (14) and (29) that $\dot{\tilde{x}}$ is also bounded. Then, $\tilde{x}$ is uniformly continuous. In addition, positiveness of (15) brings

$$
\begin{aligned}
V(\tilde{x}(0), \tilde{b}_2(0)) &\geq -\int_0^t \dot{V}(\tilde{x}(t), \tilde{b}_2(t)) dt \\
&\geq \int_0^t \alpha\beta(\eta_\Phi(x) + b_2 + l_1)\tilde{x}^2 dt
\end{aligned}
$$

Let $\overline{C} \triangleq \overline{\alpha}\overline{\beta}(\overline{\eta} + l_1) > 0$, then $\int_0^t \tilde{x}^2 dt \leq \frac{V(\tilde{x}(0), \tilde{b}_2(0))}{\overline{C}}$. Thus, $\tilde{x}$ is square integrable, and, from the uniform continuity

of $\tilde{x}^2$ (because $\tilde{x}$ is uniformly continuous), one can deduce that $\tilde{x}^2$ tends towards 0 when $t \to \infty$,

$$\lim_{t \to \infty} \tilde{x}(t) = 0 \qquad (30)$$

From (14), we deduce that

$$\lim_{t \to \infty} \dot{\tilde{b}}_2(t) = 0 \qquad (31)$$

In addition, a further time differentiation of $\dot{\tilde{x}}$ leads to

$$\begin{aligned}
\ddot{\tilde{x}} &= -\alpha\beta((\eta_\Phi(x) + b_2 + l_1)\dot{\tilde{x}} + \tilde{x}\dot{x}\eta'_\Phi(x) \\
&\quad + (\dot{x} - \dot{\tilde{x}})\tilde{b}_2 + (x - \tilde{x})\dot{\tilde{b}}_2)
\end{aligned}$$

Yet, $\tilde{x}$ and $\tilde{b}_2$ are bounded, while $\eta_\Phi(x) + b_2 + l_1$, and $\eta'_\Phi(x)$ are also bounded by assumption (see Section II-B). Then, from (14), $\dot{\tilde{x}}$ is bounded. Moreover, using the expression of $\dot{\tilde{b}}_2$, considering (29) and recalling that $\dot{x} = \dot{x}^r + \dot{e}$, we deduce that $\ddot{\tilde{x}}$ is bounded. As $\dot{\tilde{x}}$ is uniformly continuous and using (30), we obtain $\lim_{t \to \infty} \dot{\tilde{x}}(t) = 0$ from Barbalat's lemma ([14], Lemma 8.2). Finally, from (14),

$$\lim_{t \to \infty} \tilde{b}_2(t) = \lim_{t \to \infty} \frac{\dot{\tilde{x}} + \alpha\beta(\eta_\Phi(x) + b_2 + l_1)\tilde{x}}{\alpha\beta(x - \tilde{x})} = 0 \qquad (32)$$

Gathering (31) and (32) and recalling that, by assumption, x^r and $\dot{x}^r$ are both bounded, then, from (23), we obtain the condition (b). Finally, we can conclude with the following proposition.

Proposition 3. *The forced system (19) is λ-Uniformly Globally Asymptotically Stable (λ-UGAS). The tracking error e asymptotically converges towards 0 when $t \to \infty$.*

D. Conclusion on air mass control

We have shown that the closed-loop control law allows to address the tracking of the pressure trajectory, i.e.

$$\lim_{t \to \infty} |x^r(t) - x(t)| = 0 \qquad (33)$$

Moreover, using (7) and (8), convergence of the bias observation error (32) leads to the convergence of the generated trajectory towards the expected trajectory,

$$\lim_{t \to \infty} |x^{sp}(t) - x^r(t)| = 0 \qquad (34)$$

From (33) and (34), we can conclude on the convergence of the pressure to the expected pressure trajectory,

$$\lim_{t \to \infty} |x^{sp}(t) - x(t)| = 0 \qquad (35)$$

Recalling that pressure and air mass in the cylinder are related by (6), using (32) and (35), we obtain

$$\lim_{t \to \infty} |z^{sp}(t) - z(t)| = 0$$

Then the following proposition holds,

Proposition 4. *The closed-loop control law (12) - (13) guarantees the tracking of the air mass trajectory.*

VI. Experimental results

In this section, we illustrate the relevance of the proposed closed-loop approach with experimental results.

A. Engine setup

The engine under consideration is a 1,8L four-cylinder SI engine using direct injection technology and homogeneous combustion. The airpath consists of a turbocharger with monoscroll turbine controlled by a waste-gate, an intake throttle and a downstream-compressor heat exchanger permitting intake air temperature regulation. To take advantage of all the versatility of direct injection and turbocharging, the engine is equipped with two variable valve timing devices, for intake and exhaust valves. This engine setup is consistent with the scheme reported in Figure 1.

B. Results

The control strategy presented in this paper has been tested on an experimental test bench. Fast tip-in and tip-out are imposed to the engine to stress the improvements generated by the proposed strategy. Figure 2 compares strategy presented in [9] (strategy 1) against the proposed strategy (strategy 2) on the torque and the Air/Fuel Ratio (AFR) . The management of the AFR near the stoichiometric value is better with the new strategy, especially for tip-out. Actually, during the tip-out, the prediction of the trapped air mass sent to the AFR controller is rather poor. Good management of the AFR with strategy 2 comes from a good tracking of the fresh air charge trajectory.

Figure 3 presents the results of the control strategy proposed in that paper. Figure 3a shows the tracking of the fresh air mass in the cylinder comparing the trajectory, z^{sp}, with the reconstruction given by the observer, $\hat{z}$. The good tracking explains the efficiency of the strategy on AFR management. In Figure 3b, one can clearly see that the measurement of the intake manifold pressure, x^{meas}, tracks its reference trajectory, x^r. The set point of the throttle generating such a tracking is presented on Figure 3c. One can see the influence of the feedforward term that boosts the throttle opening area, θ_{th}^{sp}, during transients. This permits to improve torque response during transients.

Figure 4 compares the strategies for numerous torque transients. The improvements on AFR managements and thus in torque response can be seen on each transients of the experiment.

VII. Conclusion and future direction

The paper presents a new approach for controlling the airpath on a SI engine equipped with VVT actuators. The method is based on the tracking of a reference trajectory of the air mass in the cylinders. VVT actuators are considered as measured disturbances. A closed-loop control law based on the intake manifold pressure measurement is presented and its convergence its proven. The strategy is tested on test bench and improvements can be observed in AFR management (and thus, indirectly, on torque control), compared to a classical approach.

The strategy has been validated under atmospheric conditions. To extend it to turbocharging conditions, we plan to consider the change in the airpath dynamics during the transition between atmospheric and turbocharging conditions.
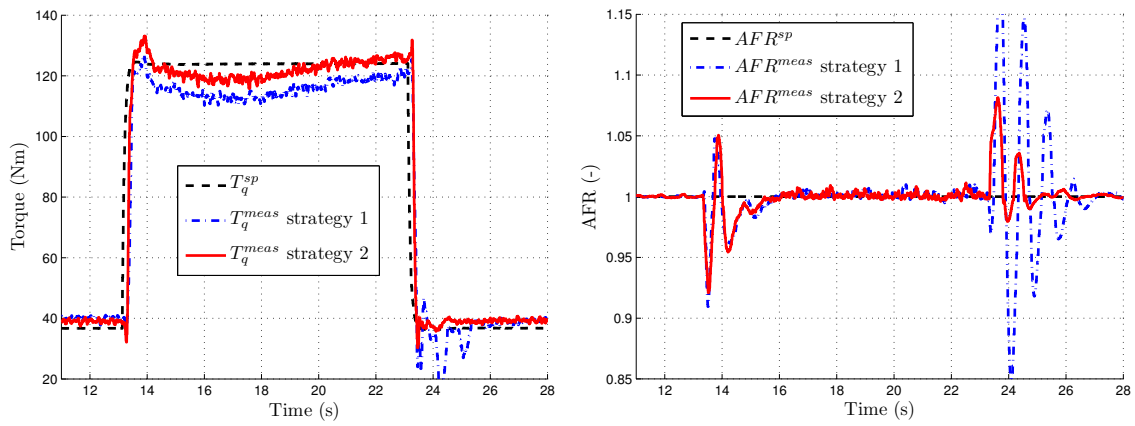
Fig. 2. Experimental results on a 4-cylinder SI engine at constant engine speed (2000 rpm). Comparison of the two AFR control strategies on torque and AFR during tip-in and tip-out. Strategy 1 : classical air mass prediction for AFR control [9], strategy 2 : proposed strategy for AFR control.
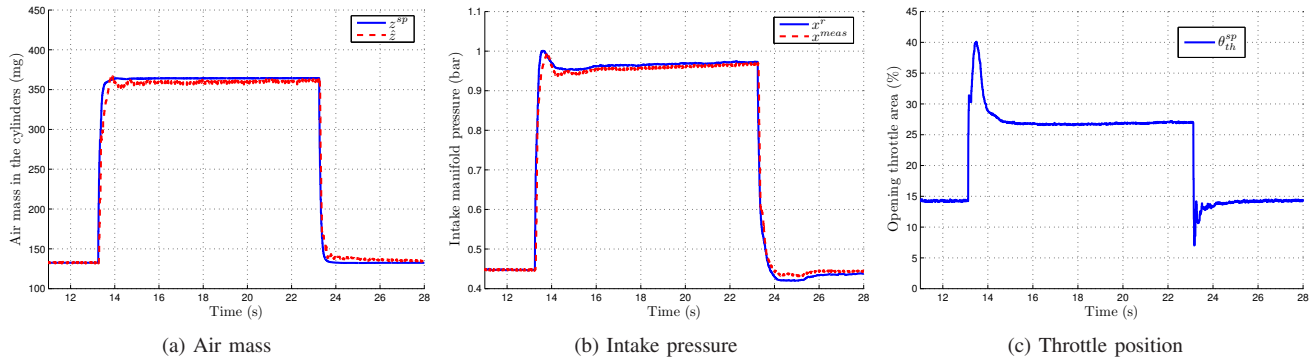

(a) Air mass   (b) Intake pressure   (c) Throttle position

Fig. 3. Experimental results on a 4-cylinder SI engine at constant engine speed (2000 rpm). Results of the proposed airpath control strategy for the same torque transients as in Figure 2.
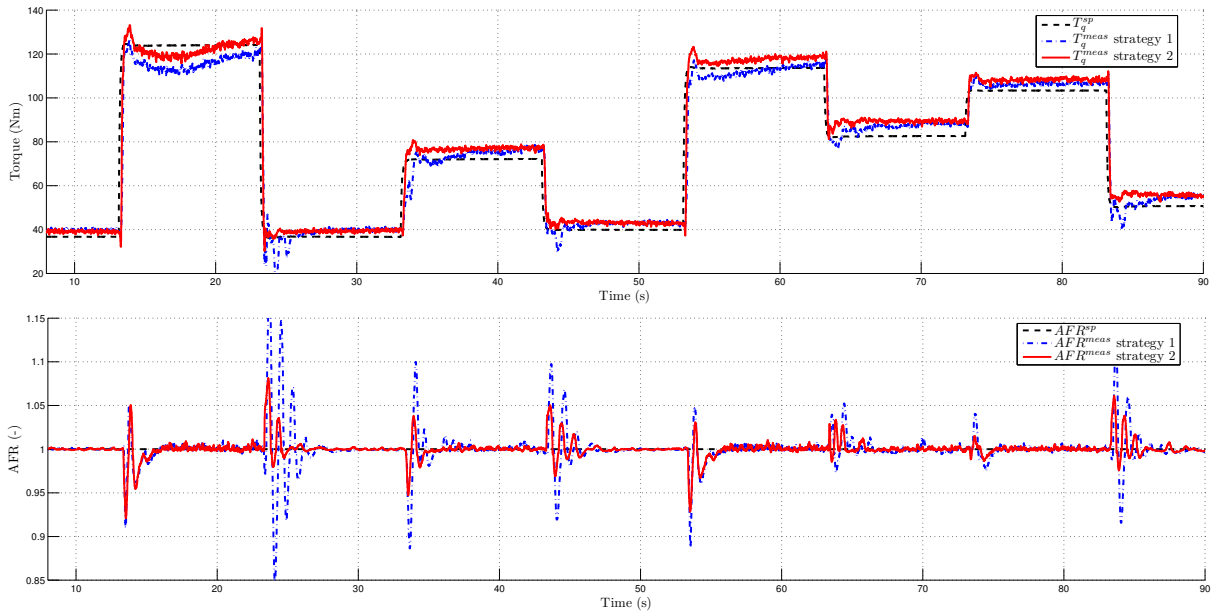

Fig. 4. Experimental results on a 4-cylinder SI engine at constant engine speed (2000 rpm). Some torque transients under atmospheric conditions. Strategy 1 : classical air mass prediction for AFR control [9], strategy 2 : proposed strategy for AFR control. Mismatch between torque set point and measurements under steady-state conditions come from inaccurate torque to in-cylinder air mass look-up table.

REFERENCES

[1] B. Lecointe and G. Monnier, "Downsizing a gasoline engine using turbocharging with direct injection," in *Proc. of SAE Conference*, no. 2003-01-0542, 2003.

[2] L. Guzzella, M. Simons, and H. Geering, "Feedback linearizing air/fuel-ratio controller," in *Control Eng. Practice*, vol. 5, no. 8, 1997, pp. 1101–1105.

[3] J. Heywood, *Internal Combustion Engine Fundamentals*. McGraw-Hill, Inc, 1988.

[4] J. Grizzle, J. Cook, and W. Milam, "Improved cylinder air charge estimation for transient air fuel ratio control," in *Proc. of the American Control Conference*, 1994.

[5] A. Chevalier, C. Vigild, and E. Hendricks, "Predicting the port air mass flow of SI engines in air/fuel ratio control applications," in *Proc. of SAE Conference*, no. 2000-01-0260, 2000.

[6] M. Jankovic, "Nonlinear control in automotive engine applications," in *in Proc. of 15th International Symposium on Mathematical Theory of Networks and Systems*, 2002.

[7] M. Jankovic, F. Frischmuth, A. Stefanopoulou, and J. Cook, "Torque management of engines with variable cam timing," in *Control Systems Magazine, IEEE*, vol. 18, 1998, pp. 34–42.

[8] A. Stefanopoulou and I. Kolmanovsky, "Dynamic scheduling of internal exhaust gas recirculation systems," in *Proc. IMECE*, vol. 61, 1997, pp. 671–678.

[9] G. Le Solliec, J. Chauvin, and G. Corde, "Experimental airpath control of a turbocharged SI engine with valve timing actuators," in *Proc. of IFAC Automotive Control*, 2007.

[10] P. Andersson and L. Eriksson, "Air-to-cylinder observer on a turbocharged SI-engine with wastegate," in *Proc. of SAE Conference*, no. 2001-01-0262, 2001.

[11] L. Guzzella and C. Onder, *Introduction to Modeling and Control of Internal Combustion Engine Systems*. Springer, 2004.

[12] A. Stotsky and I. Kolmanovsky, "Application of input estimation techniques to charge estimation and control in automotive engines," in *Control Engineering Practice*, vol. 10, 2002, pp. 1371–1383.

[13] A. Loría and E. Panteley, "Uniform exponential stability of linear time-varying systems : revisited," in *Systems & Control Letters*, vol. 47, 2002, pp. 13–24.

[14] H. Khalil, *Nonlinear Systems*. Prentice-Hall, Inc., 1992.